International Journal of Pharmaceutics: X 8 (2024) 100306

Contents lists available at ScienceDirect

International Journal of Pharmaceutics: X

journal homepage: www.sciencedirect.com/journal/international-journal-of-pharmaceutics-x

Prodigiosin hydrogel to promote healing of trauma-infected multidrug-resistant *Staphylococcus aureus* mice wounds

Xin Wang, Guangfan Meng, Zongyu Zhang, Jiacheng Zhao, Shaoyu Wang, Dongliang Hua, JingZhang *, Jie Zhang *

School of Bioengineering, State Key Laboratory of Biobased Material and Green Papermaking, Qilu University of Technology (Shandong Academy of Sciences), Jinan 250353, China

ARTICLE INFO

Keywords:
Prodigiosin
Multidrug-resistant *Staphylococcus aureus*
Antibacterial
Hydrogel
Wound healing
Inflammation

ABSTRACT

Wound infections caused by Multidrug-resistant *Staphylococcus aureus* (MRSA) have been regarded as a challenging problem in clinic for the long time. In this study, based on the excellent antimicrobial effect of prodigiosin(PG) and the ability of hydrogel dressing in terms of tissue repair and regeneration, we prepared the PG hydrogel as a treatment for the wound infection induced by MRSA. Rheological tests indicated that PG hydrogel as a semi-solid gel had good mechanical properties. In ex vitro drug permeation studies and dermatokinetic studies showed that PG hydrogel had high PG permeability and were capable of short-term retention in the skin. In addition, in vivo experiments for mouse skin wounds showed that the serum levels of inflammatory factors including IL-β and other inflammatory factors were reduced, the inflammatory infiltration of tissues was reduced, the transcript levels of genes such as COL1A1 were up-regulated at different stages of wound healing, and the relative abundance of genera such as *Desulfovibrio* was lowered after treatment with PG hydrogel, which facilitated wound healing in mice. Our study would provide a new solution to the clinical shortage of drugs for the treatment of MRSA infection and provide a research basis for improving the comprehensive values of PG.

1. Introduction

Due to the abuse of antibiotics, various drug-resistant bacteria including Multidrug-resistant *Staphylococcus aureus* (MRSA) have emerged (Martin et al., 2020). MRSA not only has different degrees of resistance to a variety of antibiotics, but also has complex resistance mechanism, which makes the treatment of its infection more difficult (Frazee et al., 2009; Cercenado et al., 2012; Parente et al., 2018). If the wound is infected with MRSA, it can impede the healing process. If untreated, the infection can spread to other parts of the body, such as the heart, lungs, bones, and joints, leads to sepsis, acute renal failure and so on. If untreated, the infection can spread to other parts of the body, such as the heart, lungs, bones, and joints (Vardakas et al., 2009; Doub et al., 2020; Martin et al., 2020; Qu et al., 2020), leads to sepsis, acute renal failure and so on (Saxena et al., 2009; Nielsen et al., 2016). MRSA has been one of the common pathogens of nosocomial and community infections since its discovery and almost worldwide.

Wound healing is usually a complex process, which includes four phases: haemostasis, inflammation, proliferation and remodelling (Guo SDiPietro LA., 2010), it is involved in the action of multiple cell populations, extracellular matrix and soluble mediators such as growth factors and cytokines (Farahpour et al., 2020).The main factor which could affect the wound healing is a prolonged period of inflammation (Eming et al., 2007). Once the skin is damaged, the colonization and growth of pathogenic microorganisms mediates the production of wound pro-inflammatory factors (Zhou et al., 2018; Rojas et al., 2002), which could cause the accumulation of immune cells such as macrophages and neutrophils, and then lead to inflammation (Wynn and Vannella, 2016). Therefore, the effective treatment for the wounds infected by MRSA is of great significance to human health.

With the increasing antibiotic resistance against bacteria, researchers are developing secondary metabolites from bacteria as new compounds against drug-resistant bacteria. PG as a natural red pigment, was mainly produced by *Serratia marcescens*, *Actinomycetes* and *Streptomyces* (Fürstner, 2003). Due to its biological activities such as anticancer (Wang et al., 2016), anti-malarial (Patil et al., 2011; Suryawanshi et al., 2015), anti-bacterial and immunosuppressive (Huh et al., 2008), PG shows great value in medical applications. Studies have

* Corresponding authors.
E-mail addresses: zhangjing@qlu.edu.cn (JingZhang), zhangjie@qlu.edu.cn (J. Zhang).

https://doi.org/10.1016/j.ijpx.2024.100306
Received 17 August 2024; Received in revised form 15 November 2024; Accepted 16 November 2024
Available online 21 November 2024

shown that PG has different degrees of inhibition on bacteria and fungi, including Gram-positive bacteria (*Staphylococcus aureus*, *Staphylococcus saprophyticus* and *Bacillus subtilis*, etc.), Gram-negative bacteria (*Escherichia coli*, *Pseudomonas aeruginosa* and *Aeromonas hydrophila*, etc.) (Ibrahim et al., 2014), fungi (*Fusarium oxysporum*, *Aspergillus flavus* and *Penicillium*, etc.) (Balasubramaniam et al., 2019). Therefore, PG has great potential as a substitute for commonly used drugs in the treatment of wound bacterial infections.

As one of the most promising materials in modern biomedicine, hydrogels show great advantage in the fields of haemostasis, tissue reconstruction, drug delivery and promotion of wound healing, due to their dynamic and reversible nature and their ability to provide a moist environment for tissues (Hamidi et al., 2008). Traditional administration methods have some drawbacks such as easy degradation, non-specific distribution, and poor drug solubility, while hydrogels have great potential in wound healing due to their high water content and better biocompatibility (Naahidi et al., 2017). Using hydrogels to carry antimicrobial substances has received widespread attention (Liu et al., 2020).

In this study, in view of the excellent antimicrobial effect of PG, it is considered to be applied to the mouse bacterial infection model to verify its anti-infection ability in order to provide the clinical basis for the application of PG in medicine.

2. Materials and methods

2.1. Materials

Kanamycin, Penicillin, Cefuroxime, Azithromycin, Ofloxacin, Doxycycline, Vancomycin, Ethylparaben, Triethanolamine (Psaitong, China), MH medium, MRSA chromogenic medium (Hopebiol, China), Carbomer-940 (Macklin, China), Glycerol (Sinopharm, China), Sodium sulfide (Xi Long Science, China), VEGFA antibody (Servicebio, China), MCP-1 ELISA test kit, TNF-α ELISA test kit, IL-6 ELISA test kit, IL-1β ELISA test kit (Lengton, China), RNA extraction kit, Reverse transcription kit, DNA extraction kit (Vazyme, China), AxyPrep DNA Gel extraction kit (Axygen Biosciences, USA).

The strain *Serratia marcescens* ZPG19 used in the experiment was preserved in the laboratory. Professor Yuqing Liu from the Institute of Animal Husbandry and Veterinary Medicine, Shandong Academy of Agricultural Sciences, provided MRSA JN62. PG was isolated from the fermentation products of *S. marcescens* ZPG19.

2.2. MRSA resistance assessment

MRSA resistance was assessed by determining the Minimum Inhibitory Concentration (MIC) of different antibiotics against MRSA JN62. The antibiotics selected for the experiment included Kanamycin, Penicillin, Cefuroxime, Azithromycin, Erythromycin, Ofloxacin, Doxycycline, Vancomycin. A series of diluted drug solution (100 μL) and 10^5 CFU/mL bacterial solution (100 μL) were added to the 96-well plate, while a negative control group (sterile broth and bacterial solution) and a blank control group (sterile broth and distilled water) were established. They were incubated at 37 °C for about 24 h, then the OD_{600} in each well was determined by Micro plate spectrophotometer (BioTek Gen5, USA). The difference between the two readings was calculated, and MICs of antibiotics were considered as the concentrations which differences in OD were less than 0.1.

2.3. Hydrogel preparation

1 g carbomer-940 as gel matrix was swelled in the appropriate distilled for 24 h, then added 1 MIC PG, 4 MIC PG and 1 MIC vancomycin. Nipagin ethyl (0.1 g) as the preservative, and glycerol (8 g) as the humectant were added. After mixing well, the pH was adjusted to neutral by adding the appropriate triethanolamine or sodium hydroxide to avoid skin irritation. The hydrogel was continuously stirred until homogeneous. Finally, the corresponding blank hydrogel, low concentration PG hydrogel, high concentration PG hydrogel and vancomycin hydrogel were obtained.

2.4. Characterization of PG hydrogel

2.4.1. Fourier transform infrared spectroscopy (FTIR)

The chemical structures of PG hydrogels were characterized using FTIR (Nicolet iS50, USA). The ATR mode was selected and the scanning range was from 4000 to 400 cm^{-1}.

2.4.2. Rheological property test

The rheological properties of the hydrogels were tested by three different methods using a rheometer (Anton Paar MCR92, Austria). (1) Rotational/steady mode, measuring shear stress-shear rate curves with shear rates from 0.1 to 1000 1/s. (2) Oscillatory/dynamic mode, measuring modulus-frequency curves with constant strain of 1 % and frequency range of 0.1–100 HZ. (3) Oscillating/dynamic mode, measuring modulus-strain curves with a constant frequency of 1 Hz and a strain range of 0.1 % to 100 %.

2.5. In vitro drug permeation

In vitro drug permeation studies were performed in a Franz diffusion cell. The skin of mice was cut down to the subcutaneous tissue without the fat layer and blood vessels and the dermis did not need to be separated from the epidermis, then placed in the Franz diffusion cell using a 50 % aqueous ethanol solution as the receptor medium. The solution was homogenized by stirring with a magnetic stirrer. At regular intervals (0.5 h, 1 h, 1.5 h, 2 h, 4 h, 6 h, 8 h, 20 h), 1 mL was removed and replaced with the corresponding aqueous ethanol solution, and the concentration of PG was measured by HPLC to plot the curve of percentage drug permeation versus time.

2.6. Dermatokinetics

Dermatokinetics studies were also carried out in a Franz diffusion cell (Alkholifi et al., 2023). One diffusion cell was used at 0.5 h, 1 h, 1.5 h, 2 h, 4 h, 6 h, 8 h, 20 h and the skin was removed for homogenization, diluted in ethanol solution and the PG concentration was determined by HPLC. The curve of drug concentration versus time was plotted. Measurement of kinetic parameters: Maximum achievable concentration (C_{max}), Time to maximum concentration (T_{max}), Area under the curve (AUC).

2.7. Establishment of wound infection model in mice

2.7.1. Mouse management and wound infection

Healthy male Kunming mice (Weight 20 ± 2 g, 3 weeks) were obtained from Pengyue Laboratory Animal Breeding Co., Ltd. (Jinan, China; experimental animal use license: SCXK (Lu) 20,140,007). Mice were fed under natural ventilation with free access of food and water. Paddings were replaced regularly during the feeding period. There were a 7-day laboratory acclimatisation period.

After acclimatisation period, hair removal treatment was performed on the mice before 24 h of modelling. The mice were anaesthetised by intraperitoneal injection of 1 % sodium pentobarbital, and the backs of the mice were depilated with 8 % sodium sulphide. The mice were anaesthetised with 1 % sodium pentobarbital, the dehairing area was disinfected and a wound of approximately 1 cm × 1 cm was made with a scalpel down to the fascial layer of the skin. 50 μL of 10^8 CFU/ mL of MRSA bacterial solution was applied evenly to the traumatic surface of the mice twice at 10 min interval. The model was successfully established if the wound showed inflammatory reactions such as redness and swelling, and increased marginal exudate, which indicated that MRSA

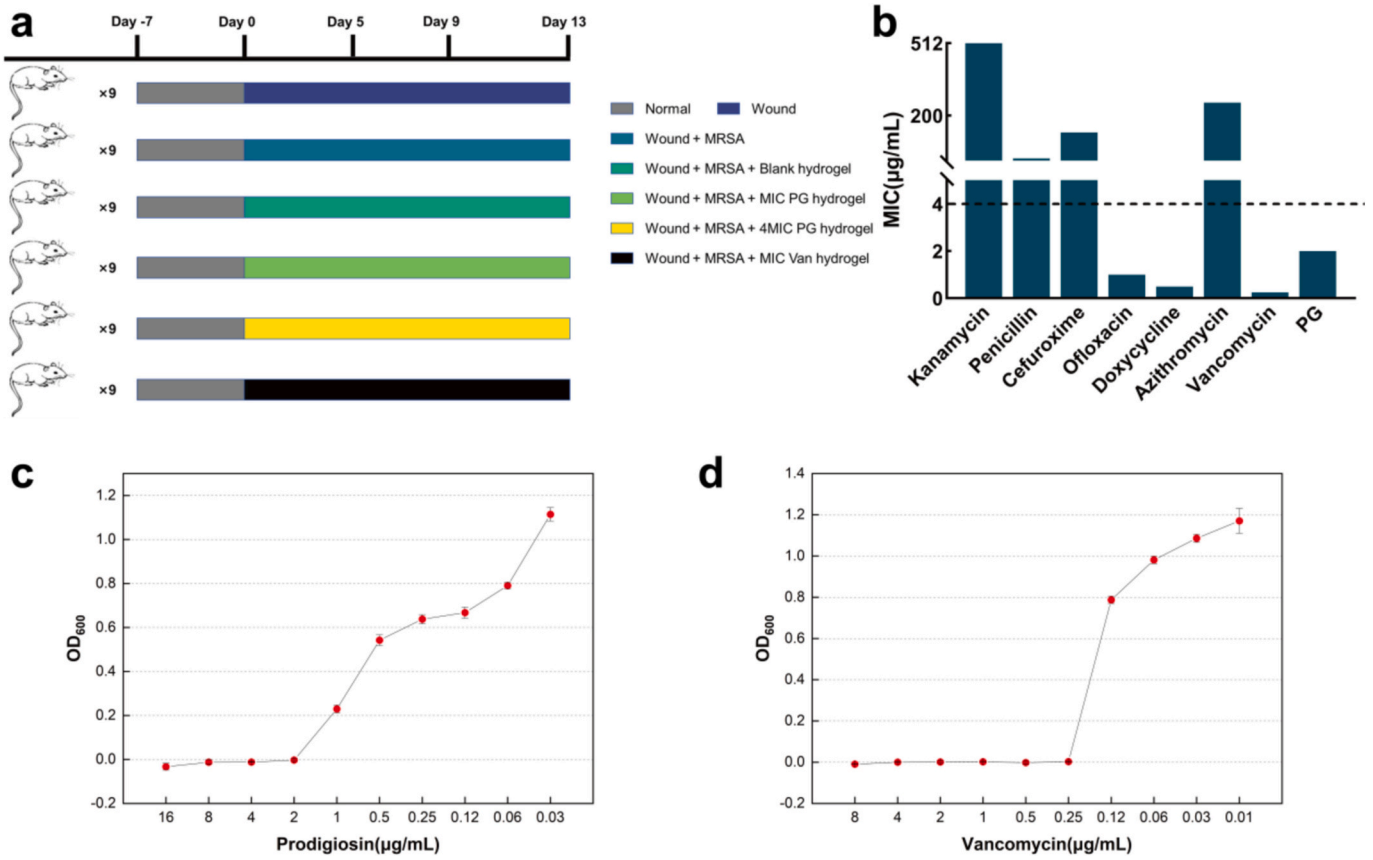

Fig. 1. (a) Experimental groups: Uninfected group (Wound), Model group (Wound + MRSA), Blank group (Wound + MRSA + Blank hydrogel), Low PG group (Wound + MRSA + MIC PG hydrogel), High PG group (Wound + MRSA +4MIC PG hydrogel) and Van group (Wound + MRSA + MIC Van hydrogel) ($n = 9$). (b) The MIC of various antibiotics against MRSA. (c) MIC of vancomycin against MRSA. (d) MIC of PG against MRSA.

strains grew on the wound after 24 h.

2.7.2. Experiment grouping and route of administration

Fifty-four Kunming mice were divided into six groups ($n = 9$) (Fig. 1a): the Uninfected group (wound created but no bacterial fluid of MRSA applied), the Model group (wound created and bacterial fluid of MRSA applied but no drug administered), the Blank group (wound infected and blank hydrogel applied), the Low PG group (wound infected and Low PG hydrogel applied), the High PG group (wound infected and high-concentration PG hydrogel applied), and the Van group (wound infected and vancomycin hydrogel applied).

After successful modelling, 1 g of the corresponding hydrogel was collected daily and applied evenly to the traumatic surface of the mice, and these mice were kept in a single cage with free access to water and food during the administration period. Three mice per group were collected on 5 d, 9 d and 13 d, then injected with 1 % sodium pentobarbital and euthanised by decapitation.

2.7.3. Assessment of wound healing

Wound were photographed on 5 d, 9 d and 13 d of the experiment and the images were then processed using Image J software to obtain the corresponding wound area. Wound closure rate was calculated as follows:

Wound closure rate (%) = (0d wound area - current wound area) / 0d wound area × 100 %.

2.7.4. Wound bacterial load count

Wound tissue from each mouse was taken and homogenized and then the diluted homogenate was inoculated onto chromogenic medium for MRSA. After incubating at 37 °C for 24 h, the colony counting was performed.

2.7.5. Histopathological analysis

We randomly selected three mice from each of the six groups and took tissue from their wounds to make tissue sections on 9 d.Tissues from wounds of 9 d mice after treatments using different hydrogels were placed in 4 % paraformaldehyde, dehydrated in ethanol, cleared in xylene, embedded in paraffin and subjected to hematoxylin and eosin (H&E) staining, Masson's trichrome (MT) staining and immunohistochemical staining with VEGFA antibody, respectively. Observations were made using a light microscope (AX-300, China). The acquired images were analysed using Image J software to estimate VEGFA expression.

2.7.6. Measurement of serum inflammatory factors

On 5 d, 3 mice per group were taken for eyeball removal and blood collection. The obtained blood was allowed to clot naturally at room temperature for 10–20 min, centrifuged at 2000 *g* for 15 min, and the serum carefully collected and stored at a − 20 °C refrigerator (if precipitate was detected prior to testing, centrifuged again). ELISA kits were used to determine levels of relevant inflammatory factors, including MCP-1, TNF-α, IL-6 and IL-1β.

2.7.7. Analysis of mRNA expression levels

Mouse tissues (30–50 mg) were collected and ground with liquid nitrogen, and total RNA was extracted from each sample using an RNA extraction kit. The concentration and purity of the RNA was determined using an ultra-micro spectrophotometer (Implen P360, China). High quality RNAs were used for the cDNA synthesis with the Reverse Transcription Kit.

Table 1
Forward and Reverse sequences sequences used in qPCR.

Gene	Forward Primer	Reverse Primer
COL1A1	CAGCGTAGCCTACATGGACC	CAAGTTCCGGTGTGACTCGT
COL3A1	AAAATTCTGCCACCCCGAAC	CAGTGCTTACGTGGGACAGT
TGF-β1	GTGGAAATCAACGGGATCAGC	GTTGGTATCCAGGGCTCTCC
VEGFA	AGGCAGACTATTCAGCGGAC	AACCGTTGGCACGATTTAAGAG
HGF	TCTGCCTGTGCCTTGACTTAG	ATGCCGGGCTGAAAGAATCA
EGF	GTCCGCTAGAGAAATGTCAATG	GCAGGAAACAAGTTCGTGACA

The expression of *COL1A1*, *CLOL3A1*, *TGF-β1*, *VEGFA*, *HGF*, *FGF-7*, *EGF* and *EGFR* gene-specific mRNA was detected by qPCR using a fluorescence quantitative PCR instrument (ABI7500, USA). Table 1 shows the forward and reverse sequences of the oligonucleotide primers. The normalization of the results was conducted using the $2^{-\Delta\Delta Ct}$ method, considering Actb as a reference gene.

2.7.8. Wound flora analysis

Total DNAs of all bacteria from the wound tissue of 5 d -mouse were extracted using the DNA extraction kit, and the V3 + V4 regions of 16S rDNA were amplified using specific barcoded primers. The primer sequences were: 341F: 5'-CCTACGGGNGGCWGCAG-3′; 806R: 5'-GGACTACHVGGGTATCTAAT-3′. Amplicons were purified using the AxyPrep DNA Gel Extraction Kit (Axygen Biosciences, USA) according to the manufacturer's instructions and quantified using the ABI StepOnePlus Real-Time PCR System (Life Technologies, USA). Purified amplicons were subjected to paired-end sequencing using standard protocols on the Illumina platform (Gidio Biotechnology, China). Sequence preprocessing and quality control were performed by paired-end ligation and chimera removal.

2.8. Statistical analysis

Differences between the experimental and control groups in this study were differentiated by statistical analyses using GraphPad Prism 6.0. Data were expressed as mean ± standard deviation (SD), and a *p*-value <0.05 was considered significantly. Significant differences between the different groups and the model group were calculated by one-way ANOVA (* $p < 0.05$, ** $p < 0.01$, *** $p < 0.001$, **** $p < 0.0001$).

3. Results and discussion

3.1. The minimum inhibitory concentration (MIC) of various antibiotics against MRSA.

The results of resistance evaluation showed that for MRSA strain number JN62 (Fig. 1b), the Minimum Inhibitory Concentration of Kanamycin was more than 512 μg/mL, Penicillin was 16 μg/mL, Cefuroxime was 128 μg/mL, the MIC of Ofloxacin was 1 μg/mL, the MIC of Doxycycline was 0.5 μg/mL, the MIC of Azithromycin was 256 μg/mL and the MIC of Vancomycin was 0.25 μg/mL (Fig. 1c). The MIC of PG was 2 μg/mL (Fig. 1d). These results showed that the strains were resistant to kanamycin, azithromycin, cefuroxime axetil and penicillin, while sensitive to vancomycin.

3.2. Characterization of PG hydrogel

As shown in the figure, Carbomer 940 acted as an excellent gel matrix with a short gel formation time and the gel state that was not altered by the addition of PG. The injectability of the PG hydrogel was also demonstrated by the ability to write through the syringe (Fig. 2a, b). Such physical properties facilitate drug delivery under minimally invasive conditions (Sangboonruang et al., 2024).

FTIR was used to characterize the PG hydrogel. The shared spectral peaks of the three gels were mainly located at 3263 cm^{-1}, 1637 cm^{-1} and 1040 cm^{-1}. The spectral peak at 3263 cm^{-1} is attributed to the O—H stretching vibration due to the higher water content in the hydrogel (Fig. 2c) (Wang et al., 2023). The spectral peak at 1637 cm^{-1} is attributed to the C═C stretching vibration in carbomer 940 and ethyl nipagin, but the intensity of the spectral peaks for the Low PG and High PG groups is slightly higher than that of the blank group due to the presence

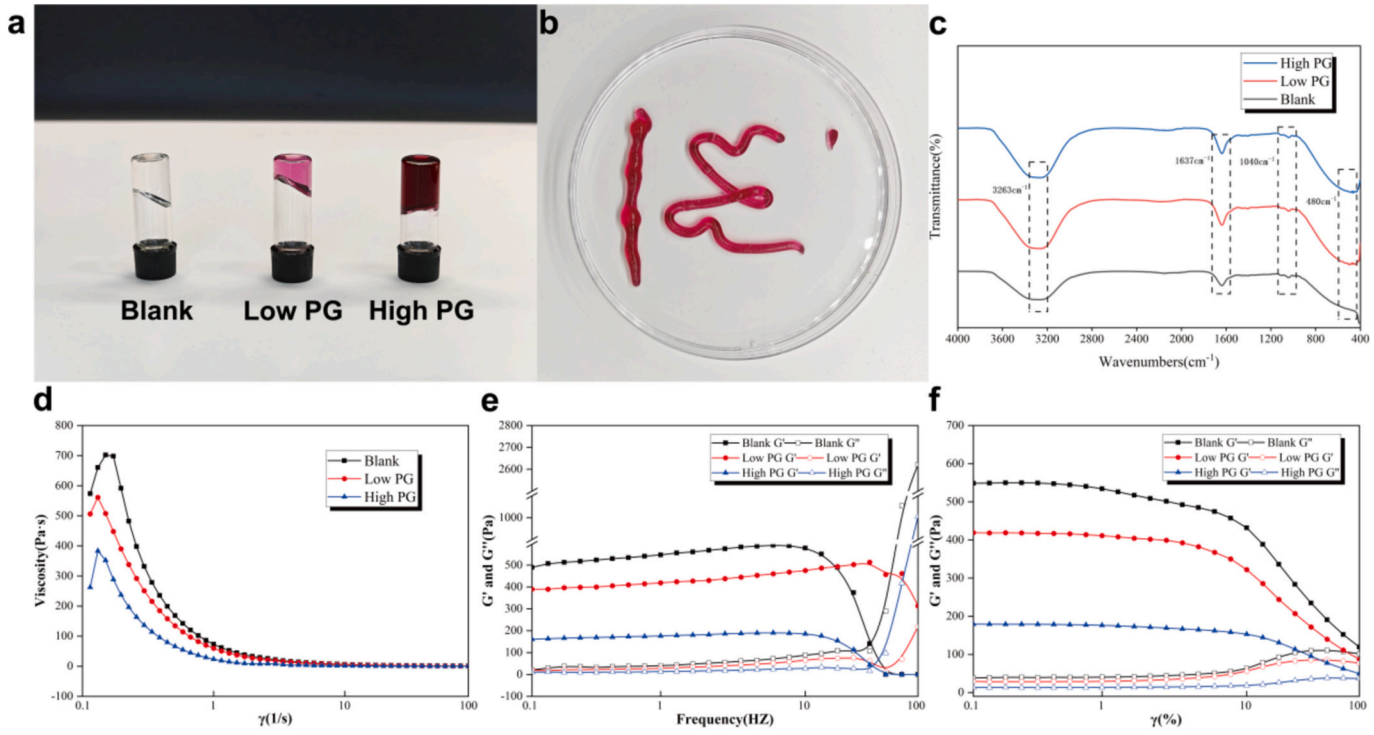

Fig. 2. Characterization of hydrogels. (a, b) Photographs of hydrogels at 37 °C. (c) FTIR spectra of hydrogels. (d) Shear stress-shear rate curves of hydrogels. (e) Modulus-frequency curves of hydrogels. (f) Modulus-strain curves of hydrogels.

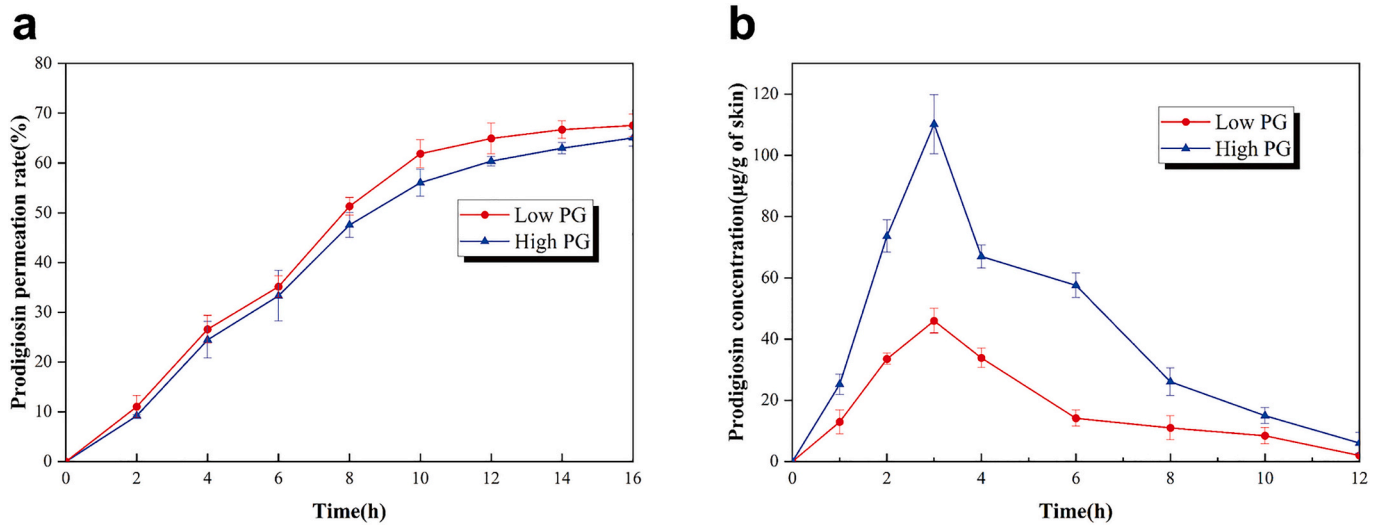

Fig. 3. (a) The curve of percentage PG permeation versus time. (b) The curve of PG concentration versus time.

of the same C═C in the tricopyrrolidine ring of PG. The consecutive small peaks at 1040 cm^{-1} are attributed to C—O, C—N and C—C stretching vibrations. Compared to the blank group, the Low PG and High PG groups showed a spectral peak at 480 cm^{-1} attributed to the C-C-C stretching vibration of PG and Glycerol. Therefore, it can be seen that PG was successfully loaded into the hydrogel.

In order to be able to understand the mechanical properties of PG hydrogel, we carried out rheological analyses of hydrogels from Blank, Low PG and High PG groups. Firstly, the viscosity of the hydrogel was assessed by measuring the change in viscosity with the change in shear rate. It can be seen that the viscosity of each group for hydrogel decreased with increasing shear rate (Fig. 2d). As the PG concentration increased, the viscosity of the hydrogel also tends to decrease. However, there was a gradual convergence of the viscosity of each group of hydrogels after the shear rate exceeded 1 1/s, indicating the shear thinning of the PG hydrogel. The ability to maintain high viscosity at low shear rates and low viscosity at high shear rates meant it was both stable under normal conditions and perfect for use in injection systems. The results of frequency scanning showed that all groups of hydrogels can maintain their G' and G" with the constant strain of 1 %, and the frequency of 0.1–10 HZ (Fig. 2e). However, when the frequency exceeded 10 HZ, the G' of each group of hydrogels decreased sharply, while the G" increased sharply, and the G" of individual groups even exceeded the G", indicating that the PG hydrogel did not have better viscoelasticity (Xiong et al., 2023). The strain scanning results showed that at a constant frequency of 1 HZ there was a linear viscoelastic region for each group of hydrogel at strains of 0.1 %–10 % and neither G' nor G" changed much (Fig. 2f). When the strain exceeded 10 %, the G' of each group started to decrease sharply and the G" increased slightly. This reflected the shear thinning property of PG hydrogel and the deformation of the microstructure under high strain (Sangboonruang et al., 2024). This property allows PG hydrogel to be applied not only to regular wounds but also to various irregularly shaped sites.

3.3. *In vitro drug permeation and dermatokinetics*

In view of the prepared hydrogel based on the excellent antimicrobial effect of PG, the drug permeation ability is one of the important factors in evaluating the performance of hydrogel materials. Therefore, we used mouse skin as a surrogate to simulate drug diffusion in a Franz diffusion cell. It can be seen that the percentage of PG permeation gradually increased in the Low PG and High PG groups, with a higher trend of drug permeation in the first ten hours and a levelling off of drug permeation after 10 h, reaching 67.55 ± 2.52 % and 65.04 ± 1.94 % permeation at 12 h (Fig. 3a). The rapid permeation of the drug helps to eliminate bacteria in the pre-infectious phase of the wound and is extremely useful in controlling wound inflammation. The carbomer gel matrix provides an efficient drug delivery system. Lower concentrations of PG have a higher permeation rate, possibly due to the smaller pores when higher concentrations of PG are added to the gel matrix (Liang et al., 2020).

Table 2
Dermatokinetic parameters of the skin drug concentration-time profile of PG in mouse skin.

Dermatokinetic parameter	Low PG	High PG
C_{max} (μg/g of skin)	45.97 ± 4.18	110.20 ± 10.89
T_{max} (h)	3	3
AUC (μg·g^{-1}·h)	212.36 ± 33.96	512.84 ± 48.48

Dermatokinetics is used to study the pattern of drug absorption, distribution and metabolism in the skin (Aggarwal NGoindi S., 2012). The drug passes through the skin and into the bloodstream, and the Low PG and High PG groups can not only eliminate the bacteria in the wound in time, but also prevent the bacteraemia caused by the infected wound. Therefore, we investigated the dermatokinetics of PG. A Franz diffusion cell was used to simulate topical administration of the drug, and the PG concentration in the skin tissue homogenate showed dynamic changes with time. As shown in the Fig. 3b, the PG released from the Low PG and High PG groups could be rapidly absorbed into the skin after administration, reaching a maximum value of 45.97 ± 4.18 μg/g and 110.20 ± 10.89 μg/g after 3 h, respectively, with the High PG group remaining at a higher concentration in the skin (Table 2). After 3 h, the drug concentration in the skin tissues all showed a decreasing trend. The calculated AUCs for the Low PG and High PG groups were 212.36 ± 33.96 μg·g^{-1}·h and 512.84 ± 48.48 μg·g^{-1}·h, respectively, indicating that the PG gels not only had a high PG permeation rate, but also facilitated the maintenance of PG concentration in the skin, which could better inhibit MRSA proliferation in the vicinity of the wound.

3.4. *PG hydrogel promotes wound healing and epithelial contraction*

As the number of treatment days increased, the wound area gradually decreased in all groups (Fig. 4a), and the wound closure rates in the Uninfected, Blank, Low PG, High PG and Van groups were significantly increased compared to the Model group ($p < 0.0001$). After treatment with a high concentration of PG hydrogel, the oedema of the infected wounds of the mice was improved, the exudate at the wound edge was

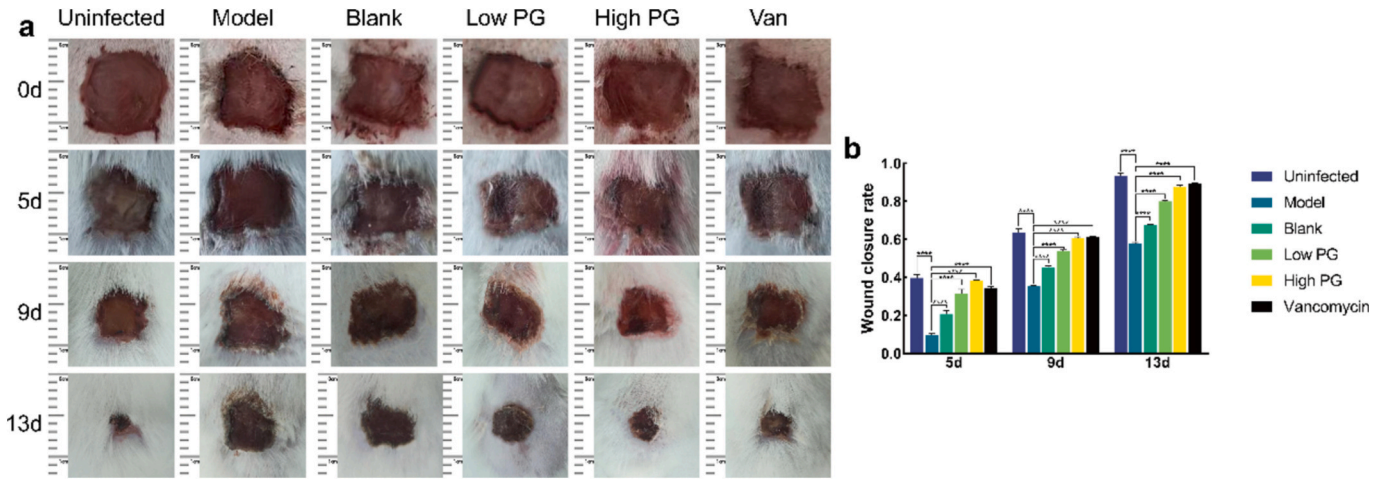

Fig. 4. Wound healing after MRSA infection of mouse wounds. (a) Relative wound area for each group of mice on days 0, 5, 9 and 13 of wound infection. (b) Statistical analysis of relative wound area.

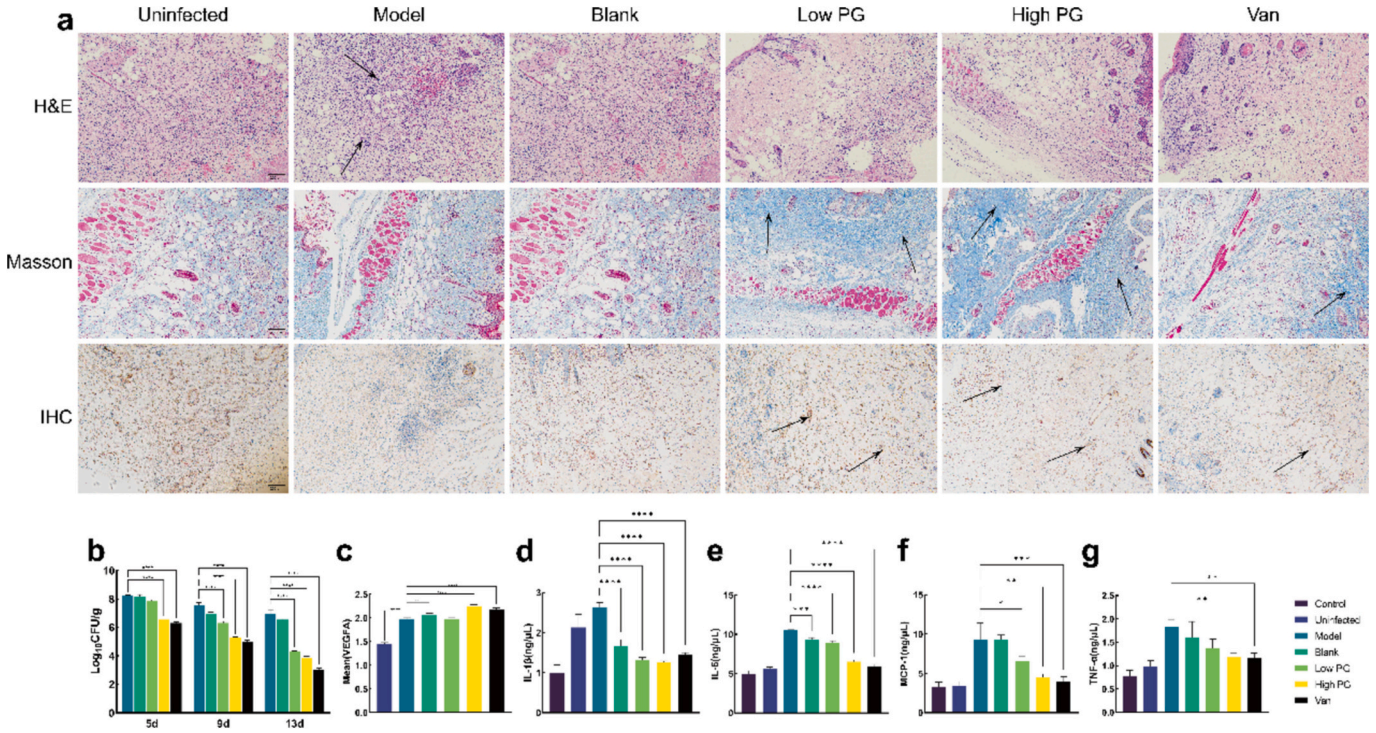

Fig. 5. (a) Microscopic observation of H&*E*-stained sections, Masson trichrome-stained sections and VEGFA immunohistochemistry-stained sections of wound tissues of each group on day 9. Scale bar = 200 μm ($n = 3$). (b) The statistics for wound MRSA load were collected for the Model group and each treatment group on days 5, 9, and 13 (n = 3). (c) Statistical analysis of VEGFA immunohistochemical staining area (n = 3). (d-g) Concentrations of IL-1β, IL-6, MCP-1 and TNF-α in the serum of mice in each group on day 5 (n = 3).

reduced, and wound was repaired remarkably, with a wound closure rate of more than 80 % (Fig. 4b), showing a very high skin regeneration advantage, indicating that the PG hydrogel had a significant effect on wound repair in mice and promoted epithelial contraction of the wounds in mice.

3.5. PG hydrogel reduces wound inflammation and promotes morphological recovery

The continued proliferation of bacteria in the wound is key to the persistence of inflammation. On the 5th, 9th and 13th days after post infection, live bacteria from the wounds of the mice were counted to assess the anti-infective ability of the different hydrogels (Fig. 5b). On the 5th day, the viable wound bacterial count was 6.55 ± 0.12 Log_{10} CFU/g in the High PG group and 6.32 ± 0.09 Log_{10} CFU/g in the Van group, which was significantly lower compared to the Model group (8.23 ± 0.05 Log_{10} CFU/g) ($p < 0.0001$). On the 9th day, the wound viable bacterial counts were 6.32 ± 0.12 Log_{10} CFU/g in the Low PG group, 5.27 ± 0.09 Log_{10} CFU/g in the High PG group, and 4.98 ± 0.15 Log_{10} CFU/g in the Van group, which were significantly lower compared to the Model group (7.56 ± 0.22 Log_{10} CFU/g) ($p < 0.0001$). On the 13th day, the wound viable bacterial counts were 4.33 ± 0.05 Log_{10} CFU/g in the Low PG group, 3.87 ± 0.13 Log_{10} CFU/g in the High PG group, and 3.03 ± 0.13 Log_{10} CFU/g in the Van group, which were significantly

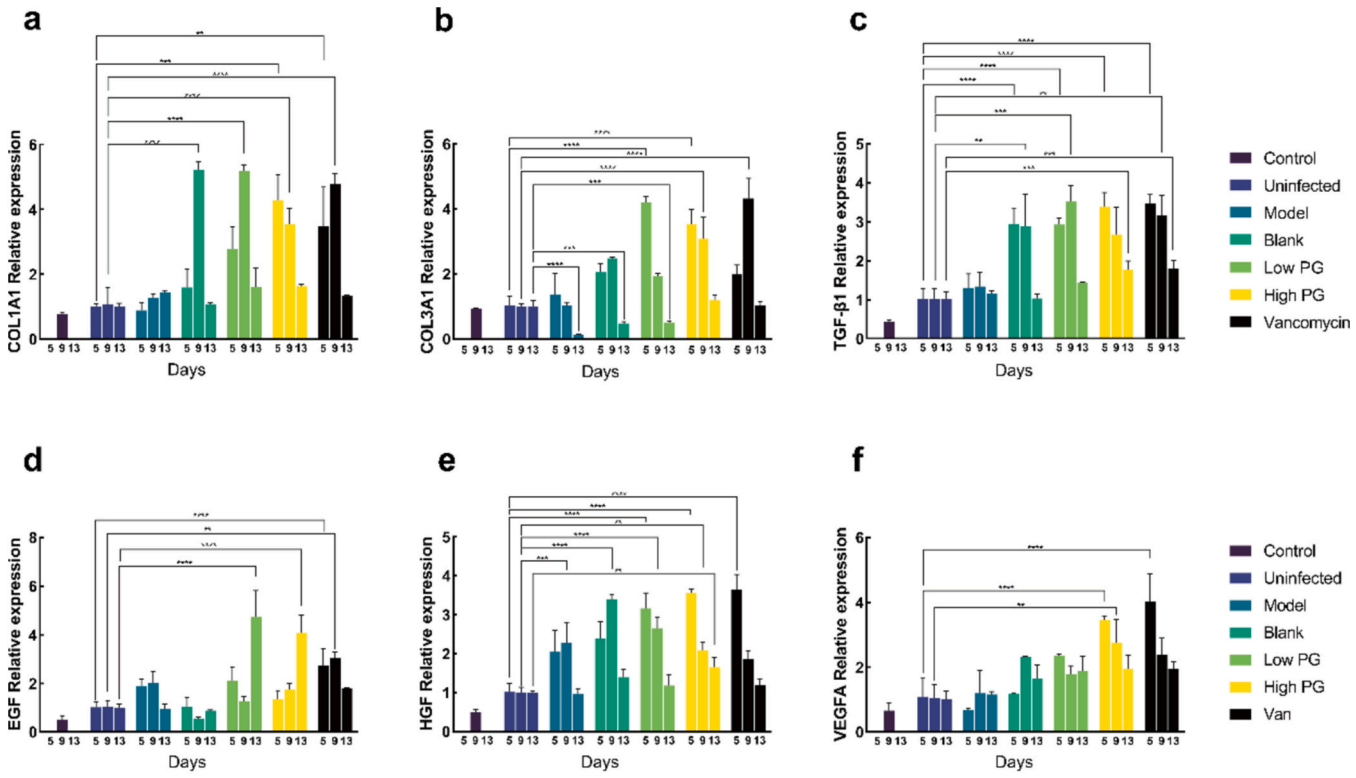

Fig. 6. mRNA expression of *COL1A1* (a), *COL3A1* (b), *TGF-β1* (c), *EGF* (d), *HGF* (e) and *VEGFA* (f) on days 5, 9 and 13 ($n = 3$).

lower compared to the Model group (7.56 ± 0.22 Log_{10} CFU/g) ($p < 0.0001$). As the treatment progresses, the PG hydrogel improved the swelling and suppuration on the wounds of the mice, and reduced the bacterial load compared to the untreated mice. Thus, PG hydrogel can reduce the bacterial count in mouse wounds to a certain extent and has a positive effect on inhibiting MRSA wound infection in mice.

Inflammation, an important stage of wound healing, which regulating the synthesis of numerous cytokines (Landén et al., 2016), However, excessive inflammatory reactions accompanied by physiological phenomena such as redness, swelling, pus, and fever (Chiu et al., 2013; Blomqvist AEngblom D., 2018), and damaging to the body and organs (Stramer et al., 2007). In hematoxylin & eosin (H&E) sections, the Model group showed more inflammatory infiltration compared to the other groups, while the High PG and Van groups had more fibroblasts with robust dermal angiogenesis but little inflammatory infiltration compared to the other groups (Fig. 5a), and neutrophils and macrophages, which were coloured blue by the dye, were not overrepresented. It was shown that the PG hydrogel had a good inhibitory effect on the pro-inflammatory response, enabling wound healing in mice to enter the proliferative phase as soon as possible. Masson trichrome (MT) staining was used to observe the deposition and arrangement of collagen around the traumatic tissue. The High PG and Low PG groups exhibited greater collagen deposition, with the neoplastic collagen fibres in the High PG group arranged in an orderly manner. In contrast, the Control and Model groups had fewer collagen fibres, which were arranged in a disordered manner (Fig. 5a). The immunohistochemical results for VEGFA in the trauma tissues of each group indicated that the Control group had significantly lower VEGFA expression than the Model group. In contrast, the High PG and Van groups had significantly higher VEGFA expression than the Model group ($p < 0.0001$) (Fig. 5c). The results indicated that PG hydrogels had a positive effect on reducing wound inflammation in mice. Additionally, they increased wound collagen expression to some extent and promote blood vessel formation.

IL-1β, IL-6, MCP-1 and TNF-α, as several typical pro-inflammatory factors (Wynn, 2007; Barrientos et al., 2008; Koh TJDiPietro LA., 2011; Mantovani et al., 2012), are undoubtedly promoted by inflammation. The level of inflammatory factors in the Model group was significantly higher than that in the Uninfected group, suggesting that MRSA in mouse wounds is the main cause of inflammation formation. The levels of IL-1β and IL-6 in the Blank, Low PG, High PG, and Van groups were significantly lower compared to the Model group (IL-6 in the Blank group: $p < 0.001$; the rest of the groups: $p < 0.0001$) (Fig. 5d, e). Meanwhile, the treatment of different hydrogels resulted in the reduction of MCP-1 levels in the serum of mice (Low PG group: $p < 0.05$, High PG group: $p < 0.01$, Van group: $p < 0.001$) (Fig. 5f), and the levels of TNF-α were equally significantly reduced in the High PG group and the Van group ($p < 0.01$) (Fig. 5g). It demonstrated that PG hydrogel reduced serum inflammatory factors in mice and had a significant anti-inflammatory effect against inflammation induced by wound infection with MRSA.

3.6. PG hydrogel upregulates wound healing-related cytokines

The efficient healing of trauma is inseparable from the work of a variety of cytokines. In addition to the interaction of cell-cell and cell matrix, all the wound-repairing stages are regulated by various growth factors and cytokines (Werner SGrose R., 2003; Barrientos et al., 2008). The relative expression of cytokines associated with wound tissue healing was examined to reveal the molecular mechanism of the hydrogels effect on the wound healing process.

With regard to collagen synthesis, we examined the expression of COL1A1 and COL3A1 in the tissues (Fig. 6a, b). There is a large amount of collagen in the extracellular matrix. And collagen type I (COL1A1), as the only component of collagen fibres, has a high percentage in connective tissue which is closely related to dermal formation and skin aging (Wang et al., 2007). Collagen type III (COL3A1) can interact with collagen type I and collagen type II in order to regulate the diameter of collagen fibres and form finer collagen fibres, which reduced the formation of hypertrophic scars, and interact with platelets in the coagulation cascade. It is an important signal molecule for wound healing

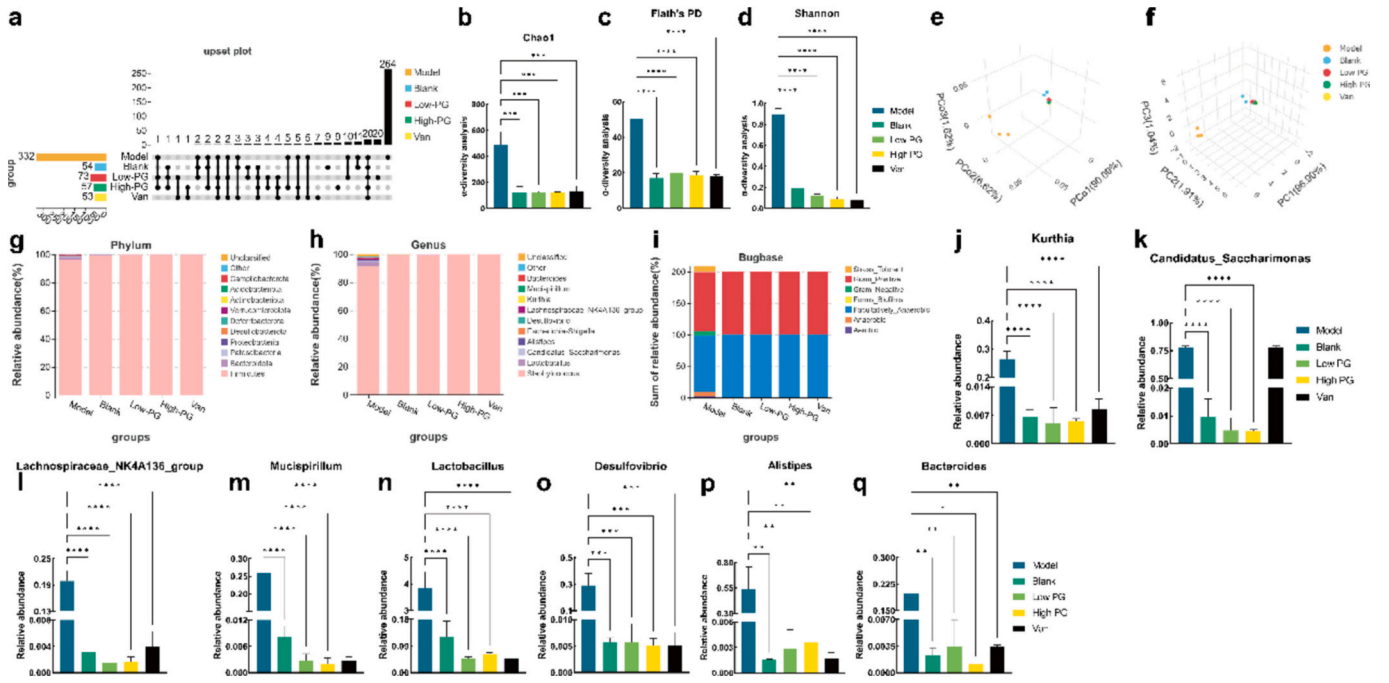

Fig. 7. Microbiological composition of mouse wounds on day 5 (n = 3). (a) OTU upset plot diagram. (b-d) Chao1, Faith's PD, and Shannon indices for α-diversity analysis. (e,f) 3D PCoA and PCA plots of β-diversity analyses. (g) Diagram of microbiological composition at the portal level. (h) Diagram of microbiological composition at the genus level. (i) Bugbase functional analysis diagram. (j-q) Relative abundance diagram of *Kurthia*, *Candidatus Saccharimonas*, *Lachnospiraceae NK4A136 group*, *Mucispirillum*, *Lactobacillus*, *Desulfovibrio*, *Alistipes* and *Bacteroides*.

(Kashiyama et al., 2012; Kuivaniemi HTromp G., 2019). COL1A1 mRNA expression was upregulated to different degrees in both the High PG and Van groups compared to the other groups on the 5th day of wound infection (High PG group: $p < 0.001$; Van group: $p < 0.01$), and oon the9th day, COL1A1 mRNA expression was significantly upregulated in the different hydrogel-treated groups compared to the Uninfected group ($p < 0.0001$). On the 5th day, COL3A1 mRNA expression was significantly upregulated in the Low PG and High PG groups ($p < 0.0001$), on the 9th day, COL3A1 mRNA expression was significantly upregulated in the High PG and Van groups (p ⟨00001). On the 13th day, COL3A1 mRNA expression was downregulated to different degrees in the Model, Blank and Low PG groups (Model group: $p < 0.0001$; Blank group: $p < 0.001$; Low PG group: $p < 0.01$). Therefore, it is concluded that the PG hydrogel induced the high expression of collagen type I and collagen type III in the wound during the pre-trauma period. The thick collagen fibres of collagen type I could help maintain the integrity of the connective tissue, making the skin stronger. Collagen type III could better maintain the elasticity of the skin. Then the interaction of collagen in the wound would accelerate the epithelial formation of the wound tissue, which could prevent the invasion of other pathogens and promote wound healing (Panagiotou et al., 2023).

With regard to cell growth, we examined the expression of TGF-β1 and EGF in the tissues (Fig. 6c, d). TGF-β1, a member of the transforming growth factor-β family, is highly expressed in the granulation tissue of trauma. It can stimulate angiogenesis, fibroblast proliferation, collagen fiber cell differentiation and matrix deposition, which could promote the transcription of COL1A1 (Falanga et al., 2002; Werner SGrose R., 2003), It has also been reported that TGF-β1-deficient mice showed slower wound repair (Brown et al., 2002). Epidermal Growth Factor (EGF) promotes mitosis in fibroblasts and keratinocytes, facilitating rapid proliferation and promoting wound healing (Werner SGrose R., 2003). TGF-β1 mRNA expression was significantly upregulated in the groups treated with different hydrogels on the 5th day ($p < 0.0001$), TGF-β1 mRNA expression was significantly upregulated in the Blank, Low PG and Van groups (Blank and Van groups: $p < 0.01$; Low PG group: $p < 0.001$) on the 9th day and TGF-β1 mRNA expression was significantly upregulated in the High PG and Van groups ($p < 0.001$) on the 13th day. It showed that the use of PG hydrogel induced sustained expression of TGF-β1 at the wound site, which had a role in wound haemostasis and fibroblast growth. EGF mRNA expression was upregulated in the Van group on the 5th day ($p < 0.01$), significantly upregulated in the Van group on the 9th day ($p < 0.0001$), and significantly upregulated in the Low PG and High PG groups on the 13th day ($p < 0.0001$). The results indicated that PG hydrogel induced a late phase of EGF expression at the trauma site, which had a promoting effect on the generation of new epidermal cells. The treatment of PG hydrogel increased the expression of EGF mRNA in the late stage of wound healing and maintained the continuous expression of TGF-β1 in the wound, which also could activate many physiological processes in the process of wound repair. The high expression of TGF-β1 also reduced the production of pro-inflammatory factors to a certain extent (Eming et al., 2007), which may also be one of the reasons for the significant anti-inflammatory effect of PG hydrogel. The high expression of EGF induced by the PG hydrogel led to the recruitment of more fibroblasts in the vicinity of the wound, thus promoting wound repair.

Hepatocyte growth factor (HGF) promotes hepatocyte mitosis, migration and proliferation of keratinocytes, and is closely related to the formation of new blood vessels. In the wound healing model of mice, it was found that the strong expression of HGF led to the wound healing (Cowin et al., 2001; Werner SGrose R., 2003). VEGFA, a member of the VEGF family, promotes the growth of vascular endothelial cells and induces vascular proliferation. With regard to angiogenesis, we examined the expression of HGF and VEGFA in the tissues (Fig. 6e, f). On the 5th day, HGF mRNA expression was significantly upregulated in the Low PG, High PG and Van groups ($p < 0.0001$), HGF mRNA expression was significantly upregulated in the Model, Blank, Low PG and High PG groups (Model group: $p < 0.001$; Blank and Low PG groups: $p < 0.0001$; High PG group: $p < 0.01$) on the 9th day, and HGF mRNA expression was upregulated in the High PG group ($p < 0.01$) on the 13th day, which suggested that in the pre-traumatic phase of traumatisation, the PG hydrogel induced the expression of HGF at the traumatic site, leading to an accelerated trauma healing process. On the 5th day, VEGFA mRNA

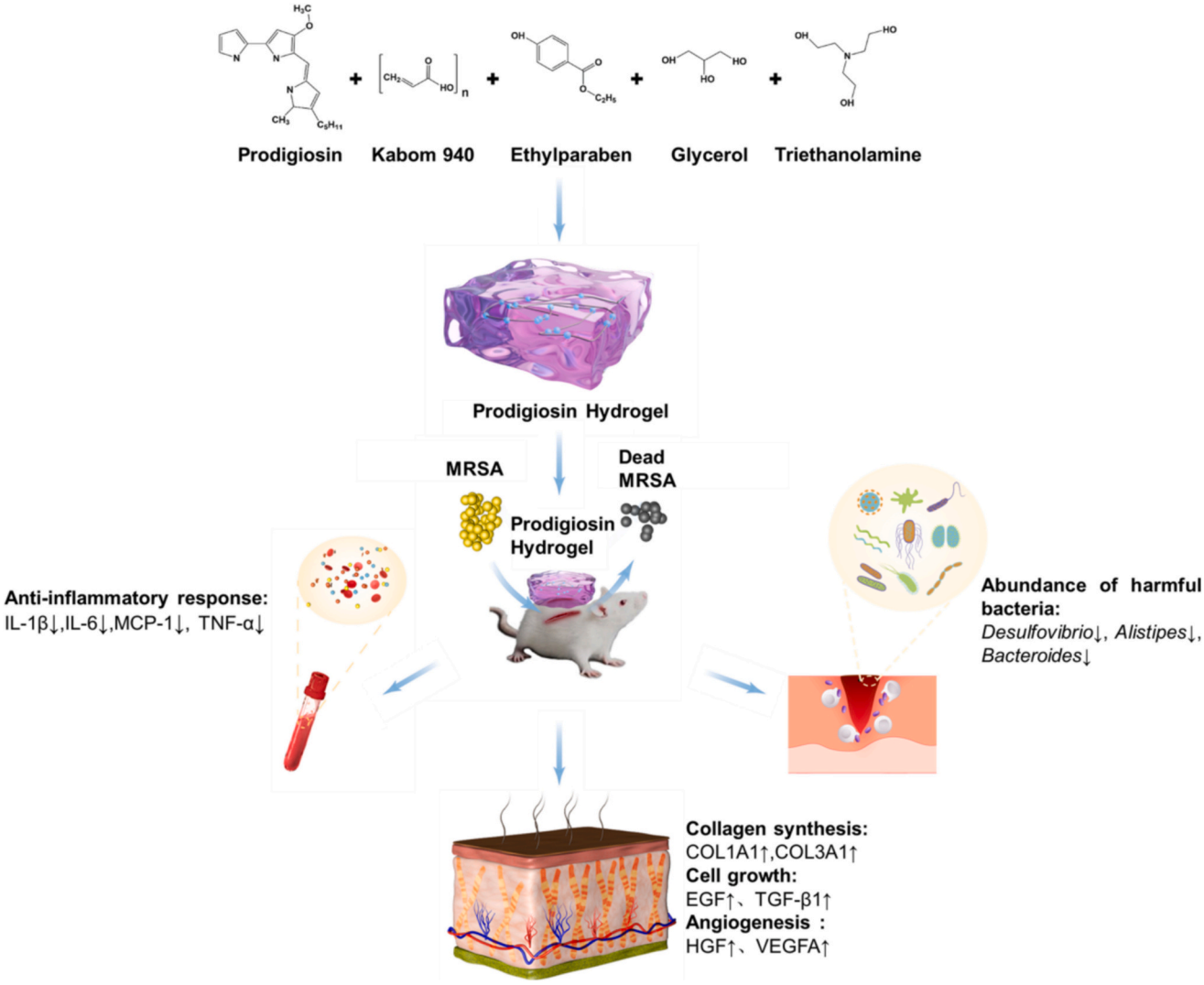

Fig. 8. PG hydrogel reduced the amounts of bacteria, reduced the content of inflammatory factors in serum, up-regulated the expression of related growth factors and cytokine mRNA in different periods, and improved the composition of wound flora in infected mice, which promoted the wound healing of MRSA-infected mice.

expression was significantly upregulated in the High PG and Van groups ($p < 0.0001$), VEGFA mRNA expression was upregulated in the High PG group ($p < 0.01$) on the 9th day. Neovascularisations in the wound provide oxygen, growth factors and immune support for the tissue and are essential for wound healing. After treatment with PG hydrogel, high expression of HGF allowed keratinocytes to proliferate and migrate near the wound, while high expression of VEGFA increased vascular permeability. After PG hydrogel treatment, the high expression of HGF and VEGFA in the wound jointly promoted the formation of wound blood vessels. The expression of VEGFA was consistent with the results of immunohistochemical area measured by Image J, which further demonstrated the positive effect of PG hydrogel on wound healing.

3.7. PG hydrogel improves the microbial composition of mouse wounds

The enrichment of multiple bacteria in the wound is an important reason for the difficulty of wound healing. After 5 days of wound infection, it was found that the microbial community of untreated mouse wound tissue was diverse and the biofilm was formed. The virulence and pathogenicity of biofilms are major obstacles to wound healing (Percival et al., 2015). To analyze the effect of the PG hydrogel on the mouse wound flora, on the 5th day of successful modelling, mouse wound tissue was collected for 16SrDNA gene sequencing to determine the microbial composition. The Upset plot (Fig. 7a) showed that the Model group contained more specific OTUs than the other groups. The results of the α-diversity analyses (Chao1, Fiath's PD and Shannon) showed (Fig. 7b-d) that the Model group had a much higher species richness than the other groups and a more homogeneous distribution of species, indicating a high diversity of flora. The results of the β-diversity analysis (PCoA, PCA) showed (Fig. 7e, f) that the compositional structure of the flora in the model group differed significantly from that of the other groups.

According to the results of the species composition analysis (Fig. 7g, h), *Firmicutes* accounted for above 90 % for all the groups at the phylum level, while the main genus of bacteria in each group was *Staphylococcus* at the genus level. A stacked plot of Bugbase phenotypic abundance (Fig. 7i) showed that the groups with higher percentages of abundance were Gram-positive bacteria and Facultative anaerobic bacteria, while the lesser Gram-negative, Forms-Biofilms and Stress-Tolerant groups of the model group also contributed to the overall phenotypic abundance. In order to further analyze the microbial composition of the mouse wound, the relative abundance of the enriched bacteria in the mouse wound was counted (Fig. 7j-q). On the 5th day, the relative abundance of the Model group and the hydrogel groups was significantly different. The abundance of *Candidatus Saccharimonas* in each group except the Van group was significantly reduced ($p < 0.0001$). The abundance of

Kurthia, *Lachnospiraceae NK4A136 group*, *Mucispirillum*, and *Lactobacillus* in each hydrogel group was significantly reduced ($p < 0.0001$). The abundance of *Desulfovibrio* was significantly reduced ($p < 0.001$), the abundance of *Alistipes* was significantly reduced ($p < 0.01$), and the relative abundance of *Bacteroides* was significantly reduced (Blank group, Low PG group and Van group: $p < 0.01$; high PG group: $p < 0.001$). In addition, although H_2S produced by *Desulfovibrio* can promote the regeneration of blood vessels, studies have shown that the release of H_2S from bacteria can enhance the resistance of species to immune-mediated killing (Toliver-Kinsky et al., 2019), which may increase the chance of MRSA survival in the wound. Although *Alistipes* can protect liver fibrosis and cardiovascular disease, it is related to the occurrence of inflammation (Parker et al., 2020). *Bacteroides* is originally derived from the gut. Once it leaves the gastrointestinal tract, infections such as abscesses, causing skin and soft tissue infections would be exacerbated (Brook, 2002). After PG hydrogel treatment, not only the load of MRSA in the wound was reduced, but also the diversity of wound flora was reduced in the early stage of trauma. PG hydrogel reduced the abundance of *Desulfovibrio*, *Alistipes* and *Bacteroides*, reduced the effect of other bacteria on wound repair, and indirectly promoted wound healing.

4. Conclusion

In summary, MRSA could lead to the occurrence of wound inflammation and delay of wound healing. The PG hydrogel reported in this study possesses good mechanical properties, penetrated the skin quickly and remained in the skin for a short period of time. In addition, PG hydrogel showed good antibacterial and anti-inflammatory properties by reducing the wound bacterial load and reducing the content of serum inflammatory factor in a mouse model. It also promoted wound healing in mice by inducing collagen synthesis, fibroblast growth and angiogenesis. In addition, it improved the microbial community of the wounds and protected the wounds from invasion by other harmful microorganisms (Fig. 8). Our work would provide new ideas for the clinical application of PG and insight into PG as an antibacterial agent to antibacterial dressings. Certainly, analyzing various cytokines and growth factors combined with protein expression for mouse wounds will make the results more rigorous. It might be one of the limitations in this study. In addition, the mice in this study spent their entire life in a small cage, and the limited living space and minimal group socialisation may have led to depression and fear. Therefore more comprehensive and rigorous animal experiments are needed to evaluate the efficacy of PG.

Research ethics approval

This work has received approval for research ethics from the Animal Care and Use Committee of the Qilu University of Technology (Shandong Academy of Sciences) and a proof/certificate of approval is available upon request.

CRediT authorship contribution statement

Xin Wang: Writing – review & editing, Writing – original draft, Validation, Methodology, Investigation, Formal analysis, Conceptualization. **Guangfan Meng:** Validation, Investigation. **Zongyu Zhang:** Supervision, Software, Data curation. **Jiacheng Zhao:** Supervision, Software, Data curation. **Shaoyu Wang:** Supervision, Software, Data curation. **Dongliang Hua:** Writing – review & editing, Investigation. **JingZhang:** Writing – review & editing, Validation, Investigation. **Jie Zhang:** Validation, Supervision, Project administration, Investigation, Funding acquisition.

Declaration of competing interest

The authors declare that they have no known competing financial interests or personal relationships that could have appeared to influence the work reported in this paper.

Data availability

Data will be made available on request.

Acknowledgements

This study was funded by the Key Innovation Project of Qilu University of Technology (Shandong Academy of Sciences) [grant number 2022JBZ01-06]; the 2023 Provincial Key R&D Plan (Rural Revitalization Science and Technology Innovation Boosting Action Plan) (2023TZXD003); and the Central Guiding Local Science and Technology Development Special Fund Project (YDZX2023006).

References

Aggarwal NGoindi S., 2012. Preparation and evaluation of antifungal efficacy of griseofulvin loaded deformable membrane vesicles in optimized guinea pig model of Microsporum canis—Dermatophytosis. Int. J. Pharm. 437 (1–2), 277–287. https://doi.org/10.1016/j.ijpharm.2012.08.015.

Alkholifi, F.K., et al., 2023. Phospholipid-based Topical Nano-Hydrogel of Mangiferin: Enhanced Topical delivery and improved Dermatokinetics. Gels 9 (3). https://doi.org/10.3390/gels9030178.

Balasubramaniam, B., et al., 2019. Exploration of the optimized parameters for bioactive prodigiosin mass production and its biomedical applications in vitro as well as in silico. Biocatal. Agricul. Biotechnol. 22. https://doi.org/10.1016/j.bcab.2019.101385.

Barrientos, S., et al., 2008. PERSPECTIVE ARTICLE: growth factors and cytokines in wound healing. Wound Repair Regen. 16 (5), 585–601. https://doi.org/10.1111/j.1524-475X.2008.00410.x.

Blomqvist AEngblom D., 2018. Neural Mechanisms of Inflammation-Induced fever. Neuroscientist 24 (4), 381–399. https://doi.org/10.1177/1073858418760481.

Brook, I., 2002. Microbiology of polymicrobial abscesses and implications for therapy. J. Antimicrob. Chemother. 50 (6), 805–810. https://doi.org/10.1093/jac/dkg009.

Brown, R.L., et al., 2002. Wound healing in the transforming growth factor-β1—deficient mouse. Wound Repair Regen. 3 (1), 25–36. https://doi.org/10.1046/j.1524-475X.1995.30108.x.

Cercenado, E., et al., 2012. Rapid Detection of Staphylococcus aureus in lower respiratory Tract Secretions from patients with Suspected Ventilator-Associated Pneumonia: Evaluation of the Cepheid Xpert MRSA/SA SSTI Assay. J. Clin. Microbiol. 50 (12), 4095–4097. https://doi.org/10.1128/jcm.02409-12.

Chiu, I.M., et al., 2013. Bacteria activate sensory neurons that modulate pain and inflammation. Nature 501 (7465), 52–57. https://doi.org/10.1038/nature12479.

Cowin, A., et al., 2001. Hepatocyte growth factor and macrophage-stimulating protein are upregulated during excisional wound repair in rats. Cell Tissue Res. 306 (2), 239–250. https://doi.org/10.1007/s004410100443.

Doub, J.B., et al., 2020. Salvage Bacteriophage Therapy for a Chronic MRSA Prosthetic Joint Infection. Antibiotics 9 (5). https://doi.org/10.3390/antibiotics9050241.

Eming, S.A., et al., 2007. Inflammation in Wound Repair: Molecular and Cellular Mechanisms. J. Invest. Dermatol. 127 (3), 514–525. https://doi.org/10.1038/sj.jid.5700701.

Falanga, V., et al., 2002. Low oxygen tension stimulates collagen synthesis and COL1A1 transcription through the action of TGF-β1. J. Cell. Physiol. 191 (1), 42–50. https://doi.org/10.1002/jcp.10065.

Farahpour, M.R., et al., 2020. Accelerated healing by topical administration of Salvia officinalis essential oil on Pseudomonas aeruginosa and Staphylococcus aureus infected wound model. Biomed. Pharmacother. 128. https://doi.org/10.1016/j.biopha.2020.110120.

Frazee, B.W., et al., 2009. How Common is MRSA in Adult Septic Arthritis? Ann. Emerg. Med. 54 (5), 695–700. https://doi.org/10.1016/j.annemergmed.2009.06.511.

Fürstner, A., 2003. Chemistry and Biology of Roseophilin and the Prodigiosin Alkaloids: a survey of the last 2500 years. Angew. Chem. Int. Ed. 42 (31), 3582–3603. https://doi.org/10.1002/anie.200300582.

Guo SDiPietro LA., 2010. Factors Affecting Wound Healing. J. Dent. Res. 89 (3), 219–229. https://doi.org/10.1177/0022034509359125.

Hamidi, M., et al., 2008. Hydrogel nanoparticles in drug delivery. Adv. Drug Deliv. Rev. 60 (15), 1638–1649. https://doi.org/10.1016/j.addr.2008.08.002.

Huh, J.-E., et al., 2008. Immunosuppressive effect of Prodigiosin on Murine Splenocyte and Macrophages. Biomol. Ther. 16 (4), 351–355. https://doi.org/10.4062/biomolther.2008.16.4.351.

Ibrahim, D., et al., 2014. Prodigiosin - an antibacterial red pigment produced by Serratia marcescens IBRL USM 84 associated with a marine sponge Xestospongia testudinaria. J. Appl. Pharm. Sci. 4 (10), 1–6. https://doi.org/10.7324/japs.2014.401001.

Kashiyama, K., et al., 2012. miR-196a Downregulation increases the Expression of Type I and III Collagens in Keloid Fibroblasts. J. Invest. Dermatol. 132 (6), 1597–1604. https://doi.org/10.1038/jid.2012.22.

Koh TJDiPietro LA., 2011. Inflammation and wound healing: the role of the macrophage. Expert Rev. Mol. Med. 13. https://doi.org/10.1017/s1462399411001943.

Kuivaniemi HTromp G., 2019. Type III collagen (COL3A1): Gene and protein structure, tissue distribution, and associated diseases. Gene 707, 151–171. https://doi.org/10.1016/j.gene.2019.05.003.

Landén, N.X., et al., 2016. Transition from inflammation to proliferation: a critical step during wound healing. Cell. Mol. Life Sci. 73 (20), 3861–3885. https://doi.org/10.1007/s00018-016-2268-0.

Liang, Y., et al., 2020. Injectable Antimicrobial Conductive Hydrogels for Wound Disinfection and Infectious Wound Healing. Biomacromolecules 21 (5), 1841–1852. https://doi.org/10.1021/acs.biomac.9b01732.

Liu, W., et al., 2020. Synthetic Polymeric Antibacterial Hydrogel for Methicillin-Resistant Staphylococcus aureus-Infected Wound Healing: Nanoantimicrobial Self-Assembly. Drug- and Cytokine-Free Strategy. ACS Nano 14 (10), 12905–12917. https://doi.org/10.1021/acsnano.0c03855.

Mantovani, A., et al., 2012. Macrophage plasticity and polarization in tissue repair and remodelling. J. Pathol. 229 (2), 176–185. https://doi.org/10.1002/path.4133.

Martin, J.K., et al., 2020. A Dual-Mechanism Antibiotic Kills Gram-negative Bacteria and Avoids Drug Resistance. Cell 181 (7), 1518–1532.e14. https://doi.org/10.1016/j.cell.2020.05.005.

Naahidi, S., et al., 2017. Biocompatibility of hydrogel-based scaffolds for tissue engineering applications. Biotechnol. Adv. 35 (5), 530–544. https://doi.org/10.1016/j.biotechadv.2017.05.006.

Nielsen, R.T., et al., 2016. Fatal Septicemia Linked to Transmission of MRSA Clonal complex 398 in Hospital and Nursing Home. Denmark. Emerg. Infect. Dis. 22 (5), 900–902. https://doi.org/10.3201/eid2205.151835.

Panagiotou, D., et al., 2023. Role of Lactiplantibacillus plantarum UBLP-40, Lactobacillus rhamnosus UBLR-58 and Bifidobacterium longum UBBL-64 in the Wound Healing Process of the Excisional Skin. Nutrients 15 (8). https://doi.org/10.3390/nu15081822.

Parente, D.M., et al., 2018. The Clinical Utility of Methicillin-Resistant Staphylococcus aureus (MRSA) Nasal Screening to rule out MRSA Pneumonia: a Diagnostic Meta-analysis with Antimicrobial Stewardship Implications. Clin. Infect. Dis. 67 (1), 1–7. https://doi.org/10.1093/cid/ciy024.

Parker, B.J., et al., 2020. The Genus Alistipes: Gut Bacteria with Emerging Implications to Inflammation, Cancer, and Mental Health. Front. Immunol. 11. https://doi.org/10.3389/fimmu.2020.00906.

Patil, C.D., et al., 2011. Prodigiosin produced by Serratia marcescens NMCC46 as a mosquito larvicidal agent against Aedes aegypti and Anopheles stephensi. Parasitol. Res. 109 (4), 1179–1187. https://doi.org/10.1007/s00436-011-2365-9.

Percival, S.L., et al., 2015. Biofilms and Wounds: an Overview of the evidence. Adv. Wound Care 4 (7), 373–381. https://doi.org/10.1089/wound.2014.0557.

Qu, X., et al., 2020. Biodegradable Zn–Cu alloys show antibacterial activity against MRSA bone infection by inhibiting pathogen adhesion and biofilm formation. Acta Biomater. 117, 400–417. https://doi.org/10.1016/j.actbio.2020.09.041.

Rojas, I.-G., et al., 2002. Stress-Induced Susceptibility to Bacterial Infection during Cutaneous Wound Healing. Brain Behav. Immun. 16 (1), 74–84. https://doi.org/10.1006/brbi.2000.0619.

Sangboonruang, S., et al., 2024. Multifunctional poloxamer-based thermo-responsive hydrogel loaded with human lactoferricin niosomes: in vitro study on anti-bacterial activity, accelerate wound healing, and anti-inflammation. Int. J. Pharm.: X. https://doi.org/10.1016/j.ijpx.2024.100291.

Saxena, A.K., et al., 2009. The impact of nasal carriage of methicillin-resistant and methicillin-susceptiblestaphylococcus aureus(Mrsa & Mssa) on vascular access-related septicemia among patients with type-ii diabetes on dialysis. Ren. Fail. 24 (6), 763–777. https://doi.org/10.1081/jdi-120015679.

Stramer, B.M., et al., 2007. The inflammation–fibrosis link? a jekyll and hyde role for blood cells during wound repair. J. Invest. Dermatol. 127 (5), 1009–1017. https://doi.org/10.1038/sj.jid.5700811.

Suryawanshi, R.K., et al., 2015. Mosquito larvicidal and pupaecidal potential of prodigiosin from Serratia marcescens and understanding its mechanism of action. Pestic. Biochem. Physiol. 123, 49–55. https://doi.org/10.1016/j.pestbp.2015.01.018.

Toliver-Kinsky, T., et al., 2019. H_2S, a Bacterial Defense Mechanism against the Host Immune Response. Infect. Immun. 87(1).doi:10.1128/iai.00272-18.

Vardakas, K.Z., et al., 2009. Incidence, characteristics and outcomes of patients with severe community acquired-MRSA pneumonia. Eur. Respir. J. 34 (5), 1148–1158. https://doi.org/10.1183/09031936.00041009.

Wang, Q., et al., 2007. RNAi-mediated inhibition of COL1A1 and COL3A1 in human skin fibroblasts. Exp. Dermatol. 16 (7), 611–617. https://doi.org/10.1111/j.1600-0625.2007.00574.x.

Wang, Z., et al., 2016. Prodigiosin inhibits Wnt/β-catenin signaling and exerts anticancer activity in breast cancer cells. Proc. Natl. Acad. Sci. 113 (46), 13150–13155. https://doi.org/10.1073/pnas.1616336113.

Wang, Y., et al., 2023. Sodium alginate/poly(vinyl alcohol)/taxifolin nanofiber mat promoting diabetic wound healing by modulating the inflammatory response, angiogenesis, and skin flora. Int. J. Biol. Macromol. 252. https://doi.org/10.1016/j.ijbiomac.2023.126530.

Werner SGrose R., 2003. Regulation of Wound Healing by Growth Factors and Cytokines. Physiol. Rev. 83 (3), 835–870. https://doi.org/10.1152/physrev.2003.83.3.835.

Wynn, T.A., 2007. Cellular and molecular mechanisms of fibrosis. J. Pathol. 214 (2), 199–210. https://doi.org/10.1002/path.2277.

Wynn, T.A., Vannella, K.M., 2016. Macrophages in Tissue Repair, Regeneration, and Fibrosis. Immunity 44 (3), 450–462. https://doi.org/10.1016/j.immuni.2016.02.015.

Xiong, Y., et al., 2023. Hydrogelation of TPGS for locoregional combination therapy of cancer. Chem. Eng. J. 451. https://doi.org/10.1016/j.cej.2022.138889.

Zhou, J., et al., 2018. Bacteria-responsive intelligent wound dressing: Simultaneous In situ detection and inhibition of bacterial infection for accelerated wound healing. Biomaterials 161, 11–23. https://doi.org/10.1016/j.biomaterials.2018.01.024.